Hall coefficient and resistivity of thin polycrystalline Cu films-contributions of band structure



1990 J. Phys.: Condens. Matter 2 1795

(http://iopscience.iop.org/0953-8984/2/7/010)

J. Phys.: Condens. Matter **2** (1990) 1795–1805. Printed in the UK

# Hall coefficient and resistivity of thin polycrystalline Cu films—contributions of band structure

J Gogl, J Vancea and H Hoffmann
Institut für Angewandte Physik, Universität Regensburg, Universitätsstrasse 31, 8400 Regensburg, Federal Republic of Germany

Received 2 February 1989, in final form 19 April 1989

**Abstract.** Polycrystalline Cu films were produced on Cr-precoated glass substrates in the thickness range 2–40 nm at $T = 300$ K. *In situ* measurements of transversal Hall coefficient and resistivity were carried out as a function of film thickness. The thickness dependence of the film structure was investigated by transmission electron microscopy and electron diffraction. While the thickness-dependent resistivity is consistent with free-electron models, the behaviour of the Hall coefficient measured at very low thicknesses (3–10 nm) is in striking qualitative contrast to the predictions of such models. This is explained by taking into account the anisotropic band structure of Cu with respect to surface and grain boundary scattering and the change in the density of states at very low thicknesses.

## 1. Introduction

The thickness dependence of electrical resistivity and Hall coefficient of thin films is described by the standard model of Fuchs [1] and Sondheimer [2] with the following assumptions.

(i) The structure of the film material is completely isotropic with conduction electrons of only s symmetry (free electrons).

(ii) Surface scattering at the plane-parallel film surfaces is considered by a specularity parameter $p$ independent of incidence angle.

This standard free-electron model predicts a monotonic increase in resistivity with decreasing reduced thickness $d/l_0$ (figure 1($a$)). The Hall coefficient discussed here thoroughly with respect to its sign should decrease with decreasing thickness according to figure 1($b$). The quantitative amount of this general behaviour is controlled by the specularity parameter $p$. Incorporating the effects of grain boundary scattering [3–6] and of surface roughness [7] does not change this picture qualitatively.

While the measured thickness dependence of the resistivity of Cu films is at least in qualitative accordance with these predictions, this is not the case with the few existing measurements of the Hall coefficient as a function of film thickness. In [8] a decrease in the negative Hall coefficient of copper films down to a thickness of 10 nm according to the standard theory of free electrons (figure 1($b$)) is reported; this was also noticed in [9]. The value of the Hall coefficient at a large thickness of 100 nm, however, was not in agreement with the free-electron value of $-7.4 \times 10^{-11}$ m$^3$ C$^{-1}$ but rather resembled the bulk value of copper ($-5.4 \times 10^{-11}$ m$^3$ C$^{-1}$).

0953-8984/90/071795 + 11 $03.50 

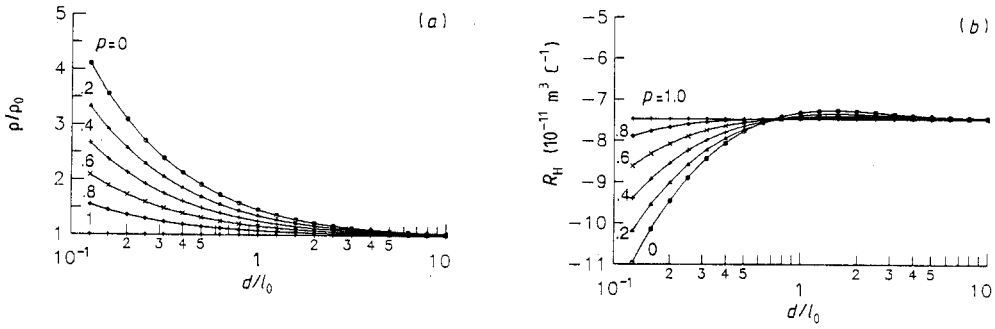


**Figure 1.** (*a*) Normalised resistivity $\rho/\rho_0$ and (*b*) Hall coefficient $R_H$ as functions of reduced thickness $d/l_0$ in the standard Fuchs–Sondheimer model, where $l_0$ is the mean free path of bulk material and $p$ the specularity parameter.

Measurements in [10], however, showed a marked qualitative deviation of the Hall coefficient of Cu films from the Fuchs–Sondheimer model for a thickness of less than 10 nm, which is still unexplained. Similar behaviour was found in [11] for K films and in [12] for Na films.

Reliable measurements of the Hall coefficient in the thickness range below 15 nm together with a careful analysis of film structure as a function of thickness are thus necessary to understand this puzzling behaviour.

## 2. Experimental details

The preparation of the Cu films and all measurements of conductivity and Hall coefficient were performed in a vacuum deposition apparatus at a pressure of $5 \times 10^{-7}$ Pa.

*In situ* measurements of the resistivity and the Hall coefficient were computer controlled. Two permanent magnets with opposite field directions were moved over the sample position by a stepping drive, providing a magnetic field of about 0.5 T. The Hall voltage was measured by the lock-in technique; this was only possible after stopping evaporation, as the magnets concealed the sample.

To obtain continuous Cu films on glass substrates at thicknesses far less than 10 nm, Cr (Maerz, 99.9%) was predeposited at a maximum mean thickness of about 1 nm and a sheet resistance $R_{sq}^{Cr}$ of at least 0.3 MΩ. Thus it was possible to produce stable Cu films with a thickness of 2 nm and a resistivity of 40–50 μΩ cm. The sheet resistance $R_{sq}$ of the couple consisting of the Cr deposit and the Cu layer was always lower than 100 Ω in the concerned thickness range. The Cr coatings used with mean thicknesses $d < 1$ nm must be regarded as discontinuous films. Therefore, contributions from the Cr underlayer to the conductivity and Hall coefficient of the Cu layer are negligible. This was also predicted in [13] in an effective-medium model and was confirmed in preceding experiments. Only at a Cr thickness of 1.7 nm and a corresponding $R_{sq}^{Cr}$ of about 1000 Ω was a 10–20% reduction in the Hall coefficient of the layer couple observed, resulting from the positive Hall coefficient of a nearly continuous Cr underlayer with $R_H^{Cr} = +12.5 \times 10^{-11}$ m$^3$ C$^{-1}$ ($d = 5$ nm [14]).

Diffusion of Cr into Cu from the substrate interface is unlikely, since the very reactive Cr forms a relatively complex compound of the form $CrO_x(OH)_y . nH_2O$ ($x \simeq y \simeq 1$,

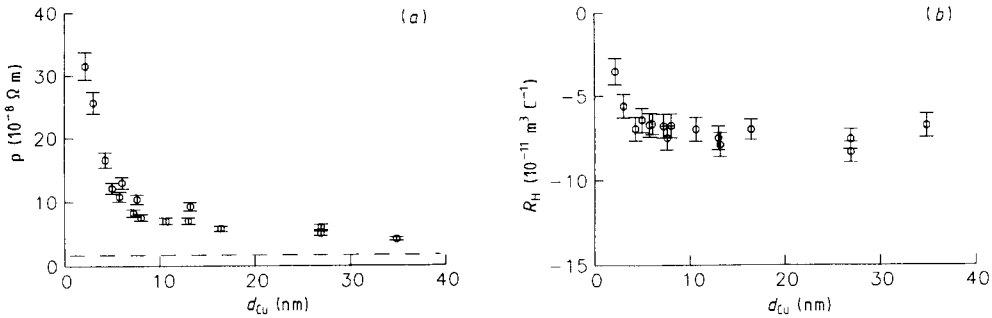


**Figure 2.** (*a*) Resistivity $\rho$ and (*b*) Hall coefficient $R_H$ of Cu monolayers prepared on Cr-precoated glass substrates as functions of Cu thickness ($T$ = 300 K): ---, resistivity $\rho_0$ of coarse-grained bulk material.

$n < 1$) with the permanent water contamination layer of the substrate, as was demonstrated in [15]. Thus, we conclude that our Cr film deposited in advance, which is about one monolayer thick, is almost totally bound to the glass substrate. Diffusion of Cr into Cu should lead to a continuous change in the Hall coefficient during or after the evaporation process; this was not observed. Moreover the Hall coefficient of thin Cu films in the range between 4 and 10 nm is independent of the thickness of the underlying Cr layer, which varies from 0.2 to 1.2 nm.

## 3. Experimental results

The thickness dependences of the Hall coefficient and resistivity were recorded in two different ways to test the influence of sample preparation.

(i) Cu films of definite thickness were evaporated in a single process as *monolayers*. The measurements were performed thereafter for the given thin film. The accuracy of the experimental values is approximately 5%, limited by the error of the absolute value of the film thickness.

(ii) Cu films were produced as *multilayers* by successive evaporation of single layers with constant thicknesses in the range 1–13 nm on the same substrate. Measurements were performed after each evaporated layer of the system. As the relative change in film thickness can be registered much more accurately by the quartz microbalance used than can the absolute film thickness, the relative thickness dependence of Hall coefficient is determined with an accuracy of 2–3%.

### *3.1. Cu monolayers*

Figure 2 shows the resistivity $\rho$ and Hall coefficient $R_H$ of Cu monolayers, prepared on glass substrates precoated with Cr at $T$ = 300 K, as a function of Cu thickness $d_{Cu}$. At a thickness of about 3 nm, the value of $\rho$ is 30–40 $\mu\Omega$ cm whereas, on substrates not treated with Cr, comparably low values are reached only when $d_{Cu} \geq 10$ nm. For thicknesses between 2 and 15 nm the resistivity decreases very rapidly with increasing Cu thickness (figure 2(*a*)), which is a consequence of several factors: the decreasing influence of surface scattering; the decreasing influence of grain boundary scattering due to grain

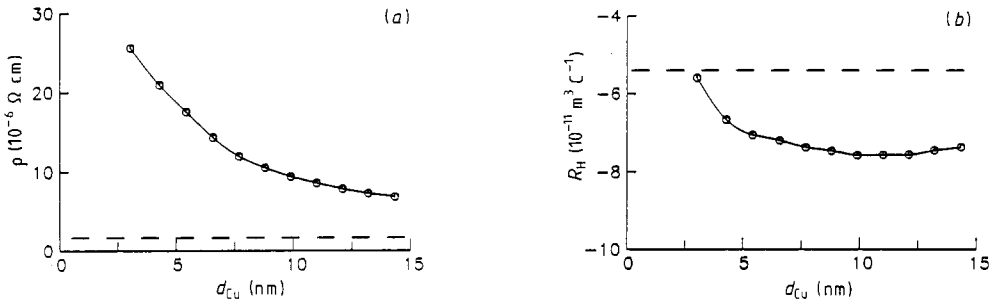


**Figure 3.** (*a*) Resistivity and (*b*) Hall coefficient $R_H$ of a Cu multilayer on Cr-precoated glass substrate as functions of Cu thickness ($T$ = 300 K); single-layer thickness, 1 nm; Cr deposit, 0.9 nm): ---, $\rho_0$ and $R_{Hb}$ for coarse-grained material.

growth; the decreasing influence of macroscopic surface roughness or film inhomogeneities. The resistivity $\rho_0$ of coarse-grained bulk material ($T$ = 300 K) is shown by a broken line for comparison.

The Hall coefficient measured simultaneously with the resistivity does not show any remarkable thickness dependence between 10 and 40 nm, lying at an $R_H$-value of $-7.4 \times 10^{-11}$ m$^3$ C$^{-1}$ for free electrons. At thicknesses decreasing from 15 to 2 nm the Hall coefficient $R_H$ (figure 2(*b*)) exceeds this value by 40%. This behaviour is qualitatively inconsistent with the Fuchs–Sondheimer theory (figure 1(*b*)).

### *3.2. Cu multilayers*

Figure 3 shows the thickness dependence of resistivity $\rho$ and Hall coefficient $R_H$ of a Cu film produced stepwise, with thicknesses of 3 nm for the first layer and 1 nm for each of the successive 10 layers. The substrates were precoated with 0.9 nm of Cr, which resulted in a sheet resistance $R_{sq}^{Cr}$ of about 1 MΩ.

The Hall coefficient (figure 3(*b*)), which is nearly constant in the thickness range between 10 and 15 nm exceeds the value for free electrons with decreasing thickness. This remarkable behaviour, which is already known from Cu monolayers (figure 2(*b*)) is thus confirmed with a relative error of the measured thickness dependence of about 2%. The resistivity $\rho$ (figure 3(*a*)) decreases with increasing number of layers in a way comparable with that of monolayers.

### *3.3. Analysis of film structure*

The thickness dependence of the film structure was controlled by electron transmission micrographs and diffraction patterns. The micrographs did not show any holes or cracks even for the thinnest removable films with $d$ = 8 nm. Moreover, if holes were present in the thickness range below 8 nm, this should result in a 'Fuchs-like' decrease in the Hall coefficient with increasing hole density as was predicted in [16] and shown in [17] for granular Au–$SiO_2$ films and in [18] for Cu–$SiO_2$ films. This is just the opposite of what was observed. Diffraction patterns obtained in the thickness range between 8 and 35 nm reveal the FCC ring system of polycrystalline Cu films, the quantitative analysis of the ring intensities showing no preferential orientation of crystallites within an experimental error limit of 15% [19].

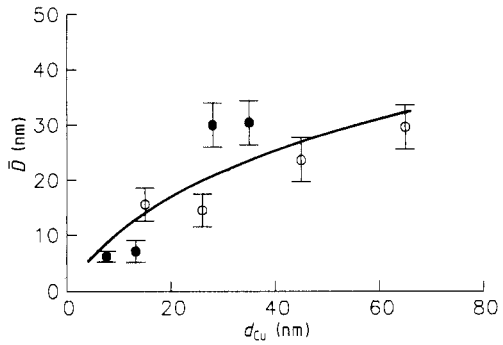


**Figure 4.** Mean crystallite diameter $\bar{D}$ of Cu monolayers (●) and multilayers (○) with single-layer thicknesses 3.7 nm, 3.2 nm, 6.0 nm and 13 nm from left to right: ——, interpolation curve according to equation (1).

The thickness-dependent mean crystallite size $\bar{D}$ was determined from electron micrographs. The results obtained for Cu monolayers and Cu multilayers are given in figure 4 as a function of film thickness $d_{Cu}$ together with the following fitted interpolation curve:

$$\bar{D} = 17.6\,\text{nm}\,\ln(1 + d_{Cu}/12.4). \tag{1}$$

Cu monolayers and multilayers show an increase in grain diameter with increasing film thickness in the range between 10 and 30 nm. The grain sizes of multilayer films correspond roughly to those of monolayers, and consequently their lateral extension exceeds by a factor of 3–4 the limiting thickness of the single-layer components. The surface roughness of the Cu films was investigated by the replica technique. The amplitude $h$ of crystallite-induced macroscopic surface roughness is also thickness dependent with $h = 8$ nm for $d = 100$ nm, and $h = 5$ nm for $d = 25$ nm; this decreases to hardly resolvable values for $d \leqslant 10$ nm.

## 4. Discussion

### *4.1. Extended free-electron models*

In figures 5(*a*) and 5(*b*) the resistivity $\rho$ and Hall coefficient $R_H$, respectively, of Cu monolayers (cf figure 2) are compared with a standard free-electron model. The full curve in figure 5(*a*) is obtained by fitting an extended Mayadas–Shatzkes model to the experimental points. The surface scattering according to [1], the thickness dependence of grain size (equation (1)) and the macroscopic surface roughness [7] were taken into account. As a result of the fitting procedure the four parameters $l_0$, $p$, $h$ and $T$ were determined as follows: background-scattering mean free path $l_0 = 26$ nm; specularity $p = 0.45$; macroscopic surface roughness amplitude $h = 2.0$ nm; transmission $T = 0.7$ of grain boundaries. These describe the experimental values fairly well.

The fitting parameters given above have only a qualitative significance. A quantitative evaluation cannot be performed owing to the limited accuracy of the experimental parameters (film thickness, grain size and surface roughness) involved (see [5] and figure 4). The calculation of the Hall effect in the present case of a thickness-dependent film structure was performed within the same model using the parameter set obtained from the fit of the resistivity dependence. The result is a strong qualitative deviation from the measured values for thicknesses less than 15 nm (figure 5(*b*)). It can be shown in

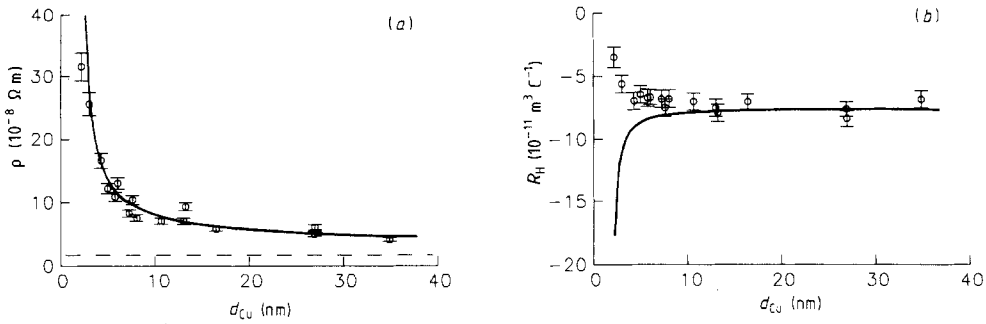


**Figure 5.** (*a*) Resistivity $\rho$ and (*b*) Hall coefficient $R_H$ of Cu films as functions of thickness $d_{Cu}$ (the curves in both (*a*) and (*b*) give the fits according to a standard model of free electrons, i.e. the Mayadas–Shatzkes model) ($\rho_0 = 1.68\ \mu\Omega$ cm; $T = 300$ K): ---, resistivity of macrocrystalline Cu.

general that all extended free-electron models are confined to values of $R_H \leqslant -7.4 \times 10^{-11}\ m^3\ C^{-1}$ [19]. Thus, free-electron models are also not capable of describing the bulk Hall coefficient $R_H^{Cu} = -5.4 \times 10^{-11}\ m^3\ C^{-1}$. Their widespread use, however, may be connected to the interesting fact that, for thick Cu polycrystalline films, $R_H^{Cu}$ nearly coincides with the free-electron value of $-7.4 \times 10^{-11}\ m^3\ C^{-1}$. This will be discussed below.

### *4.2. Anisotropic band structure of polycrystalline metals*

In contrast to the resistivity, the Hall coefficient depends more sensitively on the band structure of the film material and thus on the symmetry of the conduction electrons. This is obvious from the relations for resistivity and Hall coefficient in monocrystalline Cu under low-field conditions:

$$\sigma_0 = \frac{e^2}{12\pi^3\hbar} \int \tau(\boldsymbol{k}) v(\boldsymbol{k})\, \mathrm{d}S \tag{2a}$$

$$R_H = \frac{12\pi^3}{e} \int \tau^2(\boldsymbol{k}) v^2(\boldsymbol{k}) \overline{\left(\frac{1}{\chi}\right)}(\boldsymbol{k})\, \mathrm{d}S \Big/ \left(\int \tau(\boldsymbol{k}) v(\boldsymbol{k})\, \mathrm{d}S\right)^2. \tag{2b}$$

The conductivity $\sigma_0$ and Hall coefficient $R_H$ are determined by three parameters:

(i) the relaxation time $\tau(\boldsymbol{k})$ of the conduction electrons;
(ii) the velocity $v(\boldsymbol{k})$ at the Fermi surface;
(iii) the curvature $\overline{(1/\chi)}(\boldsymbol{k})$ of the Fermi surface.

The Hall coefficient is more sensitive to the anisotropy of band structure, since $\tau(\boldsymbol{k})$ and $v(\boldsymbol{k})$ enter the expression for $R_H$ in quadratic form and in the expression for $\sigma_0$ only in a linear form. The Hall coefficient is only influenced by *qualitative* changes in the predominant scattering process [20–23].

Simplified free-electron models are therefore replaced by the concept of an anisotropic band structure, which is necessary also in the case of polycrystalline films, since 'In microcrystalline materials the radial distribution function shows the main features as found in an ordered material' [24]. Lattice order is not destroyed in a similar way as

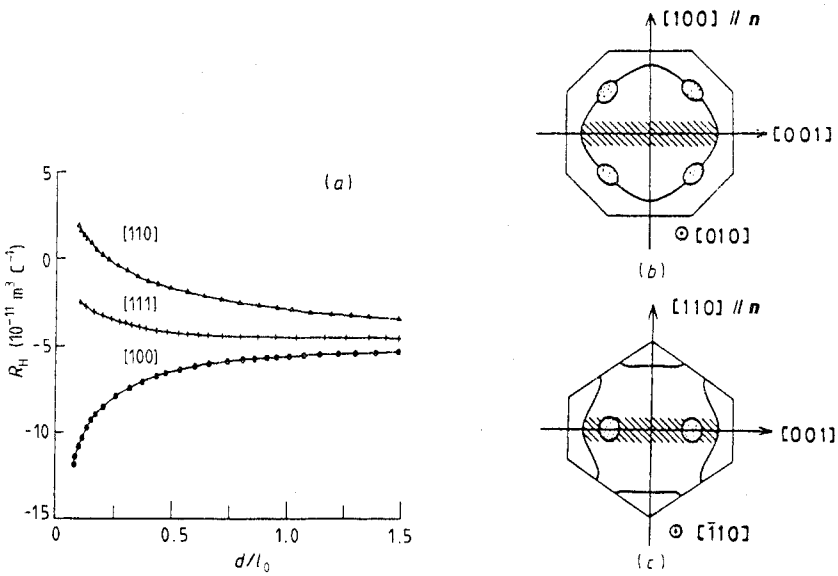


**Figure 6.** (*a*) Hall coefficient $R_H$ as a function of reduced thickness $d/l_0$ ($l_0$ is the mean free path of bulk Cu) according to [26] for differently oriented Fermi surfaces with respect to the surface normal; diffuse surface scattering was assumed ($p = 0$). (*b*), (*c*) Differently oriented Fermi surfaces of Cu with respect to the film surface normal ***n***: hatched areas mark electrons moving in the film plane and contributing mainly to conductivity and the Hall coefficient.

in melted material, where free-electron concepts are more appropriate for describing the Hall coefficient [25].

### *4.3. Thickness dependence of $R_H$ from the viewpoint of anisotropic band structure*

The thickness dependence of the Hall coefficient for the polycrystalline Cu films discussed here is determined by the dominance of one of the following scattering processes:

(i) dominant surface scattering;
(ii) dominant grain boundary scattering.

Dominant background scattering is expected only for coarse-grained thick films ($d, \bar{D} > 100$ nm) and therefore is not relevant for the films discussed in this paper. For coarse-grained films, the bulk value of $R_{Hb} = -5.4 \times 10^{-11}$ m$^3$ C$^{-1}$ at 300 K has to be expected [20–23].

### *4.4. Dominant surface scattering—monocrystalline Cu films*

As a basis for discussion, figure 6 shows the thickness dependence for monocrystalline Cu films with differently oriented lattice directions along their surface normal, calculated in [26].

Surface scattering mainly reduces the relaxation time of electrons having wavevectors with large $k_n$-components. Thus the conductivity and Hall coefficient are determined by electrons moving in the film plane and possessing the largest relaxation times. For the [100]-oriented Fermi surface (figure 6(*b*)), electrons with mainly s symmetry ('belly'

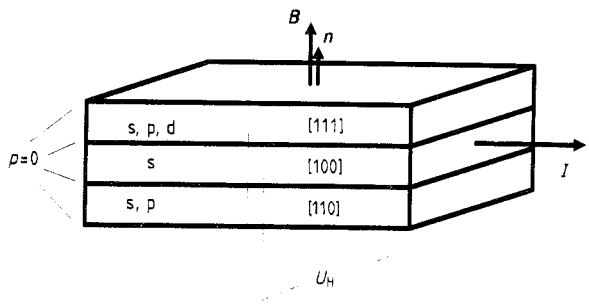


**Figure 7.** Substitute configuration of a polycrystalline film used for discussing the influence of anisotropic band structure on the thickness dependence of Hall coefficient, $I$ is the current, $\boldsymbol{B}$ is the magnetic field, $U_H$ is the Hall voltage, [111], [100] and [110] are the lattice orientations of each layer with respect to the surface normal $\boldsymbol{n}$ (diffuse scattering at layer boundaries was assumed ($p = 0$)) and s, p and d are the symmetry components of electrons moving in the respective layer planes.

electrons) are responsible for $\rho$ and $R_H$, and 'neck' electrons at the Brillouin boundary with a large $k_n$-component are strongly scattered at the surfaces. The resulting thickness dependence of $R_H$ is thus quite similar to that of free-electron models (figure 1(*b*)). If, however, the [110] direction of the Fermi surface is normal to the film surface (figure 6(*c*)), the decisive electrons moving in film plane are not only of s but also of p symmetry; the resulting thickness dependence (figure 6(*a*)) now contrasts sharply with that known from free-electron models.

### *4.5. Dominant surface scattering—polycrystalline Cu films*

Electron diffraction shows a random orientation of crystallites of the prepared Cu films. A rigorous treatment of surface and grain boundary scattering incorporating the full Fermi surface geometry would be very complex and has not yet been tackled. The limits of dominant surface and grain boundary scattering may, however, be discussed by substitution of the polycrystalline film with an arrangement of three monocrystalline layers, each having the thickness $d$ of the real film (figure 7). The Fermi surfaces of the individual layers are [111], [110] and [100] oriented. The total Hall coefficient of the configuration is calculated according to [27]:

$$R_H^G = d^G(R_H^{100}\sigma_{100}^2 d_{100} + R_H^{110}\sigma_{110}^2 d_{110} + R_H^{111}\sigma_{111}^2 d_{111})/(\sigma_{100}d_{100} + \sigma_{110}d_{110} + \sigma_{111}d_{111})^2 \tag{3}$$

with $R_H^{100}$, $R_H^{110}$ and $R_H^{111}$ as the Hall coefficients of the individual layers with thicknesses $d_{100}$, $d_{110}$ and $d_{111}$ and conductivities $\sigma_{100}$, $\sigma_{110}$ and $\sigma_{111}$. The total thickness of the configuration is $d^G = d_{100} + d_{110} + d_{111} = 3d$. Equation (3) corresponds to a three-band model. As surface scattering of [100] belly electrons affects $R_H$ quite differently from that of [110] belly electrons and [111] neck electrons, simple two-band models are not applicable in the case of surface scattering. With the assumption that $d_{100} = d_{110} = d_{111}$ and $\sigma_{100} = \sigma_{110} = \sigma_{111}$ we obtain the simple result

$$R_H^G = \tfrac{1}{3}(R_H^{100} + R_H^{110} + R_H^{111}). \tag{4}$$

The calculation of $R_H$ for each layer within the semi-classical treatment of diffuse surface scattering ($p = 0$) according to [26] yields a total Hall coefficient

$$R_H^G = \tfrac{1}{3}(R_H^{100} + R_H^{110} + R_H^{111}) \simeq -5 \times 10^{-11}\ \mathrm{m^3\ C^{-1}} \tag{5}$$

which is nearly constant in the range $d/l_0 = 0.1$–$1.5$ and contrasts the expected free-electron behaviour of figure 1(*b*) in the same range.

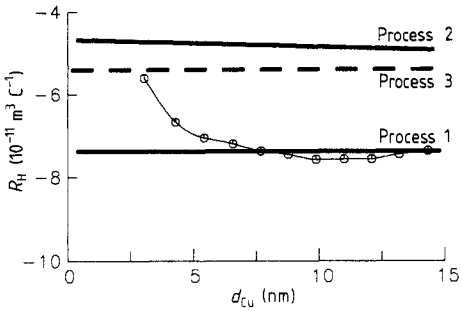


**Figure 8.** Change from dominant grain boundary to dominant surface scattering determining the thickness dependence of $R_H$ of polycrystalline Cu films in the case of anisotropic band structure: ○, experimental values for a Cu multilayer film; ——, – – –. values of $R_H$ in the limits of dominant grain boundary scattering for process 1, dominant surface scattering interpolated according to [26] for process 2 and dominant isotropic surface scattering for process 3.

In the thickness range $d \leqslant 4$ nm the quantisation of the $k_n$-component as

$$k_n = (\pi/d)N_n \qquad N_n = 1, 2, 3, \ldots \tag{6}$$

must be taken into account, as has been done for resistivity in [28]. The density of states of the electrons moving in the film plane is reduced with decreasing film thickness, as $k_n = 0$ is not allowed. These electrons, which determine mainly the Hall coefficient and conductivity, are increasingly scattered at the surfaces because of their enhanced $k_n$-component. As a consequence, anisotropic semi-classical surface scattering according to [26] assumes an increasingly isotropic character. An isotropic $\tau(\boldsymbol{k})$, however, in connection with the real Fermi surface of Cu, should also lead to $R_H \simeq -5.2 \times 10^{-11}$ m$^3$ C$^{-1}$ [20]. Therefore the consideration of the anisotropic band structure of Cu explains the experimental $R_H$-values of very thin Cu films, which are in striking contrast to predictions of free-electron models (figure 2(*b*)).

### *4.6. Dominant grain boundary scattering*

Because of their dominant p symmetry, 'neck' electrons are more strongly scattered by long-range lattice defects, e.g. the dislocation network of grain boundaries, than are 'belly' electrons with mainly s symmetry. This is of importance as long as the mean free path $l_0$ is comparable with or larger than the mean crystallite diameter $\bar{D}$. If grain boundary scattering is the dominant process, the ratio $\tau_n/\tau_b$ of the 'neck' electron relaxation time to the 'belly' electron relaxation times is in the range 0.1–0.25, leading to a Hall coefficient of about $-7.5 \times 10^{-11}$ m$^3$ C$^{-1}$ in two-band models [21–23, 29]. It is interesting that this value nearly coincides with the free-electron value $1/ne = -7.4 \times 10^{-11}$ m$^3$ C$^{-1}$, giving behaviour very similar to a free-electon type.

Applying this two-band concept to each layer in figure 8, we obtain

$$R_H^{100} \simeq R_H^{110} \simeq R_H^{111} \simeq R_{fe} \simeq -7.5 \times 10^{-11} \text{ m}^3 \text{ C}^{-1} \tag{7}$$

and thus $R_H^G \simeq -7.5 \times 10^{-11}$ m$^3$ C$^{-1}$. As the crystallite diameter $\bar{D}$ of the evaporated Cu films in figure 2 varies from about 5 nm at $d = 5$ nm to 30 nm at $d = 40$ nm, grain boundary scattering is nearly always dominant with the exception of smallest thicknesses

$d \leqslant 10$ nm. This explains why the value of $R_H$ is independent of film thickness in the range between 10 and 40 nm.

### *4.7. Change in dominant scattering mechanism with film thickness*

Interpreting the thickness dependence of the Hall coefficient for the whole thickness range, one has to bear in mind the change from one dominant scattering process to the other, e.g. from dominant grain boundary scattering to dominant surface scattering. If this is done with respect to anisotropic band structure, the thickness dependence in contrast to free electron models can be understood as demonstrated by figure 8. For a thickness of less than about 10 nm the change from dominant grain boundary scattering (process 1 in figure 8) to dominant surface scattering (processes 2 and 3) takes place. Dominant anisotropic surface scattering (process 2) interpolated across the crystallite orientation according to equation (12) leads to nearly the same value for $R_H$ as isotropic surface scattering according to the reduced density of electron states in the film plane (process 3).

## 5. Conclusion

The Hall coefficient of thin polycrystalline Cu films measured as a function of thickness in the range between 2 and 15 nm qualitatively contradicts free-electron models. Taking into account the actual band structure by the use of a substitute configuration for polycrystalline films explains the experimental results as a change from dominant grain boundary scattering ($d > 15$ nm) to dominant surface scattering at very small thicknesses ($d < 5$ nm). The deviation from free-electron models is caused by p and d symmetry of conduction electrons moving in the film plane and thus contributing mainly to the Hall coefficient at low thicknesses. Moreover at very small thicknesses their density of states is reduced because of quantum mechanical reasons, and surface scattering assumes an increasingly isotropic character, which is in sharp contrast to the Fuchs–Sondheimer model.

The thickness dependence of the resistivity, being almost insensitive to electron symmetry, remains nearly unchanged in comparison with free-electron models. Even for monocrystalline Cu films its qualitative behaviour is independent of the lattice orientation [26, 30]. On application of the interpolation scheme given above (see figure 7), the mean thickness dependence of resistivity is in very good agreement with the Fuchs model. Therefore the electrical resistivity of polycrystalline Cu films can be well explained with extended free-electron models.

## Acknowledgment

The authors wish to thank the Deutsche Forschungsgemeinschaft for financial support.

## References

[1] Fuchs K 1938 *Proc. Camb. Phil. Soc.* **34** 100
[2] Sondheimer E 1950 *Phys. Rev.* **80** 401

[3] Mayadas A F and Shatzkes M 1970 *Phys. Rev.* B **1** 1382
[4] Pichard C R, Tellier C R and Tosser A J 1979 *Thin Solid Films* **62** 189
[5] Reiss G, Vancea J and Hoffmann H 1985 *Phys. Rev. Lett.* **56** 2100
Vancea J, Hoffmann H and Kastner K 1984 *Thin Solid Films* **121** 201
Vancea J, Reiss G and Hoffmann H 1987 *Phys. Rev.* B **35** 6435
[6] Szczyrbowski J and Schmalzbauer K 1986 *J. Phys. F: Met. Phys.* **16** 2079
[7] Namba Y 1970 *Japan. J. Appl. Phys.* **9** 1326
[8] Wedler G and Wiebauer W 1975 *Thin Solid Films* **28** 65
[9] Chopra K L and Bahl S K 1967 *J. Appl. Phys.* **38** 3607
[10] Kinbara A and Ueki K 1972 *Thin Solid Films* **12** 63
[11] Cirkler W 1957 *Z. Phys.* **147** 481
[12] Heine K 1960 *Thesis* Clausthal
[13] Adkins C J 1979 *J. Phys. C: Solid State Phys.* **12** 3389
[14] Panchenko O A, Lutsishin P P and Ptushinskii Yu G 1969 *Sov. Phys.–JETP* **29** 76
[15] Gasgnier M and Névot L 1981 *Phys. Status Solidi* a **66** 525
[16] Juretschke H J and Landauer R 1963 *J. Appl. Phys.* **27** 839
[17] Sichel E K and Gittleman J I 1982 *Solid State Commun.* **42** 75
[18] Savvides N, McAlister S P, Hurd C M and Shiozaki I 1982 *Solid State Commun.* **42** 143
[19] Gogl J 1988 *Thesis* Regensburg
[20] Allgaier R S 1980 *The Hall Effect and Its Applications* ed. C L Chien and C R Westgate (New York: Plenum) p 375
[21] Lengeler B, Schilling W and Wenzl H 1970 *J. Low Temp. Phys.* **2** 237
[22] Dugdale J and Basinski Z 1967 *Phys. Rev.* **157** 552
[23] Barnard R D 1980 *J. Phys. F: Met. Phys.* **10** 2251
[24] Janot C 1980 *Electronic Structure of Crystal Defects and of Disordered Systems* ed. F Gautier, M Gerl and P Guyot (Les Ulis: Les Editions de Physique) p 177
[25] Künzi H U and Güntherodt H J 1980 *The Hall Effect and Its Applications* ed. C L Chien and C R Westgate (New York: Plenum) p 215
[26] Sakamoto I, Fukuhara M, Koide Y and Yonemitsu K 1985 *J. Low Temp. Phys.* **61** 281
[27] Petritz R L 1958 *Phys. Rev.* **110** 1254
[28] Tešanović Z 1987 *J. Phys. C: Solid State Phys.* **20** L829
[29] Hofmann F 1986 *Thesis* Regensburg
[30] Sambles J R 1987 *Thin Solid Films* **151** 159